Marina Unseld[1,2]
Christian Szepanski[3]
Andreas Lindermeir[3]
Wolfgang Maus-Friedrichs[1,2]
Sebastian Dahle[1,2,*]

Desulfurization of Biogas via Dielectric Barrier Discharges

The use of $CaCO_3$, $FeCl_3$, and FeOOH as powder sorbents for a plasma-based hydrogen sulfide removal from biogas mixtures was investigated. No plasma-enhanced surface reactions were observed during the processing. However, the high surface area provided by the powders led to an increased deposition of atomic sulfur. The dissociation of H_2S in dielectric barrier discharges was found to be effective for gas purification purposes, but limited by the backwards reaction. Medium high gas velocities in a nozzle-like plasma reactor and high retention times in a subsequent expansion vessel thus further improved the desulfurization efficiencies. Furthermore, methane production was observed, whereas the sources could not yet be fully identified.

Keywords: Biogas, Desulfurization, Dielectric barrier discharge, Hydrogen sulfide, Non-thermal plasma

Received: May 13, 2016; *revised:* December 09, 2016; *accepted:* December 15, 2016

DOI: 10.1002/ceat.201600282

1 Introduction

The occurrence of sulfur-containing compounds in gas streams usually is a problem due to their corrosive and poisonous behavior. This is an issue especially for biogas plants, where hydrogen sulfide typically appears at significant concentrations between 100 and 5000 ppmv, depending on the used substrate [1, 2].

Several techniques are available to reduce the hydrogen sulfide content in biogas. These are [2]:

– Biocatalytic desulfurization using sulfur bacteria and atmospheric oxygen which leads to the oxidation as expressed in Eqs. (1) and (2), thus forming atomic sulfur as well as sulfuric acid, which remains in the substrate.

$$2\ H_2S + O_2 \rightarrow 2\ S + 2\ H_2O \quad (1)$$

$$H_2S + 2\ O_2 \rightarrow H_2SO_4 \quad (2)$$

However, the biocatalytic desulfurization technique has several disadvantages. The temperatures, oxygen feed, and retention times have to be adjusted carefully to ensure proper desulfurization efficiencies. Typically, atmospheric air is used for the oxygen feed, thus deteriorating the quality of the biogas by nitrogen dilution. In addition, the oxygen content may temporarily exceed the explosive limit. Furthermore, the production of sulfuric acid leads to corrosion at the biogas plant. High residual H_2S concentrations require this technique to be combined with additional purification methods.

– Bioscrubbers combine a wet gas scrubber operated with sodium hydroxide solution that is regenerated by sulfur bacteria in a separate vessel. This technique enables residual H_2S concentrations in the range of 50 ppmv. However, the operational efforts are much higher than with all other techniques.

– Adding iron salts to the fermenter leads to a precipitation of iron sulfides within the substrates, see Eqs. (3) and (4). The residual H_2S concentrations for this technique vary between 50 and 300 ppmv. For H_2S values below 50 ppmv, a significant excess of iron salts is necessary, associated with notable expenses and problems with the disposal of the fermentation residue. Thus, this technique is mainly used for primary desulfurization.

$$Fe^{2+} + S^{2-} \rightarrow FeS \quad (3)$$

$$2\ Fe^{3+} + 3\ S^{2-} \rightarrow Fe_2S_3 \quad (4)$$

– The use of activated carbon as adsorption filter leads to lower residual H_2S concentration than all other techniques. The H_2S is permanently chemisorbed via oxidation as denoted in Eq. (5). The sorbent, however, is rather expensive and can

[1]Marina Unseld, Prof. Wolfgang Maus-Friedrichs, Dr. Sebastian Dahle
s.dahle@pe.tu-clausthal.de
Clausthal University of Technology, Institute of Energy Research and Physical Technologies, Leibnizstrasse 4, 38678 Clausthal-Zellerfeld, Germany.

[2]Prof. Wolfgang Maus-Friedrichs, Dr. Sebastian Dahle
Clausthal University of Technology, Clausthal Center of Material Technology (CZM), Agricolastraße 2, 38678 Clausthal-Zellerfeld, Germany.

[3]Christian Szepanski, Dr. Andreas Lindermeir
Clausthal Institute of Environmental Technology (CUTEC), Leibnizstraße 21+23, 38678 Clausthal-Zellerfeld, Germany.

 © 2017 WILEY-VCH Verlag GmbH & Co. KGaA, Weinheim

hardly be reused. Therefore, this is the most expensive desulfurization technique currently available on the market.

$$2\,H_2S + O_2 \rightarrow \frac{1}{4}\,S_8 + 2\,H_2O \quad (5)$$

– The use of plasma discharges applied to biogas has been scientifically demonstrated with respect to the production of synthesis gas [3], usually employing thermal plasmas [4], but also non-thermal plasma discharges [5]. Plasma discharges have also been employed for H_2 production [6, 7], mostly via reforming processes [8] such as direct reforming [9], steam reforming [10] or partial oxidation [11, 12]. Quite often the plasma discharges are combined with catalysts to improve the efficiencies [13].

A possible decomposition of methane is disadvantageous for gas purification purposes [14], but this can easily occur in a plasma discharge, e.g., via oxidation or polymerization [15]. Nevertheless, plasma discharges have been proven to be promising for the conditioning of biomethane by Sekine and co-workers [16]. They used dielectric barrier discharges (DBDs) and low-energy pulsed electric discharge to dissociate the hydrogen sulfide, thus producing elemental sulfur. While the DBD setup was found to be most promising for desulfurization purposes, the other discharge produced synthesis gas from biomethane with higher efficiencies.

The endothermic process of H_2S dissociation within a plasma has already been studied for pure H_2S [17, 18], the reaction enthalpies have been determined to be 300 kJ mol^{-1} H_2S [19]. However, this process has mostly been investigated at low pressures, e.g., at 20 kPa by Gutsol et al. [20]. The dissociation was found to take place more effectively at high temperatures [21], but sufficient efficiencies were gained only in combination with other systems, so far [22, 23]. Furthermore, DBDs are able to oxidize H_2S towards H_2SO_4 [24] and to induce reactions with surfaces [25]. The use of a packed-bed reactor, however, only enhanced the dissociation via the gases' residence time [26]. Nevertheless, some catalysts have been employed to enhance the dissociation of H_2S towards the production of atomic sulfur [27].

In an earlier study, the effect of DBD plasma on a gas stream of 20 vol % of H_2S in atmospheric air was investigated [28]. Whereas an empty reactor led to the deposition of atomic sulfur at the reactor walls and the formation of small amounts of SO_2 within the gas stream, a powder charge of $CaCO_3$ placed inside the plasma region resulted in a removal of over 99 % of the initial H_2S content and over 98 % of the SO_2 impurities [28].

The present study employed two DBD reactors. These were designed to optimize either one of the two observed effects. The first reactor was designed to improve the use of $CaCO_3$ as well as iron salts as sorbent. This was intended to extend the previous studies on the use of powder sorbents for these purposes [28]. The second reactor was designed to extract the sulfur fastest possible from the plasma region and thus minimize the deposition of atomic sulfur at the reactor walls. Both DBD setups were tested with different feed gas mixtures to proof possible application for biogas purification.

2 Materials and Methods

Plasma treatments have been carried out employing DBD reactors optimized for gas retention times and different deposition processes. The first reactor, denoted as powder reactor in the following, was designed to store powder amounts of approx. 1 g inside the plasma region. Further, the reactor enables the extraction of powder samples after plasma treatment at different positions in the reactor for further analysis. The powder reactor is schematically presented in Fig. 1.

The reactor consists of a stainless-steel base plate with gas in- and outlet pipes having an inner diameter of 8 mm. Six vertical quick clamps (Holex 37-6625-0) ensure a tight fit of the ceramic block made from Macor® (130 × 49 × 13 mm^3, see Fig. 1 a). The ceramic acts as dielectric barrier and allows an easy maintenance, while a Viton® sealing ring prevents gas leakage. Fig. 1 b includes a partial cutaway section along the line c-c marked in Fig. 1 a, revealing the 1-mm discharge gap (area 100 × 10 mm^2). Fig. 1 c gives a more detailed view of the discharge gap as well as the countersunk high-voltage electrode at the opposite face of the ceramic block, leaving approx. 1 mm Macor® as dielectric barrier. Calcium carbonate powder (Sigma-Aldrich, > 99.95 %), iron(III) oxide-hydroxide powder (Sigma-Aldrich, catalyst grade) and iron(III) chloride hexahydrate (Sigma-Aldrich, > 97 %) served as model sorbents.

The second plasma reactor, denoted as DBD nozzle with expansion vessel, was designed to separate the deposition zone of the generated sulfur particles from the plasma zone. High velocities and thus short retention times of the gas should minimize deposition of solid material in the plasma nozzle. In the downstream cylindrical expansion vessel the gas velocities are significantly lowered. The resulting high retention times ensure that the main fraction of the sulfur deposits on the reactor walls. As depicted in Fig. 2 a, the DBD nozzle has an inner

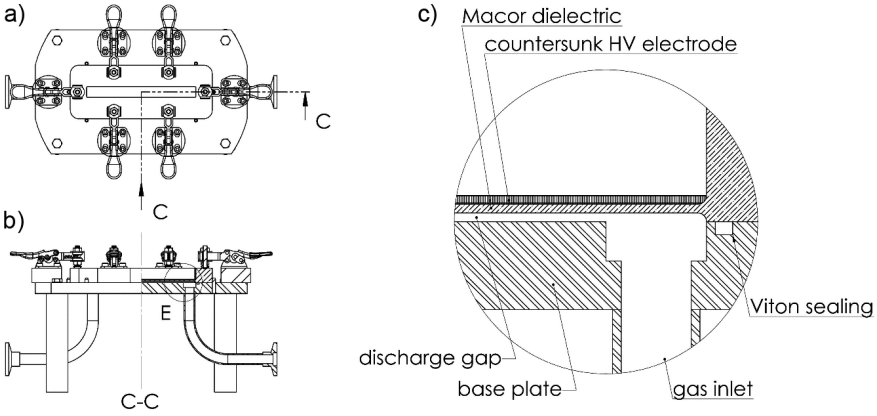

Figure 1. (a) Top view of the powder reactor, (b) side view with a part cutaway section along the line marked as c-c, (c) detail view on the cutaway section.

 © 2017 WILEY-VCH Verlag GmbH & Co. KGaA, Weinheim

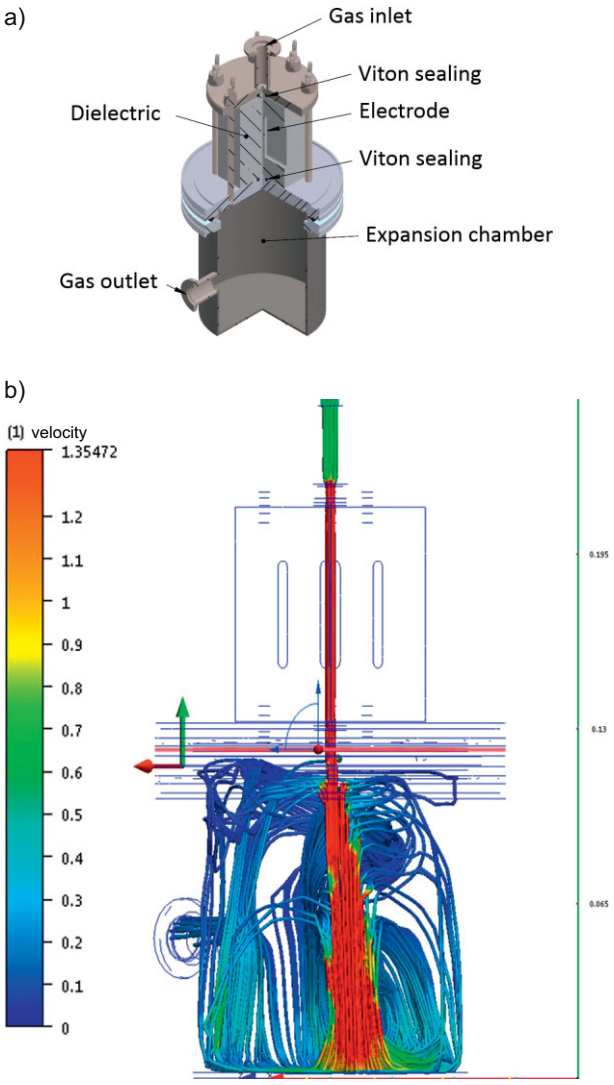

Figure 2. Sketches of the plasma nozzle (upper part) with expansion vessel (lower part) as partial section view (a) and computational flow dynamic simulation of the velocity distribution (b) with particle traces for an input flow of 0.5 SLM.

diameter of 3 mm and a length of 35 mm, the diameter of the expansion vessel is 98 mm. The velocity distribution inside the reactor has been simulated with computational fluid dynamics (Autodesk Simulation CFD) for a carrier gas flow rate of 0.5 standard liters per minute (SLM) as depicted in Fig. 2 b.

The maximum velocity of 1.35 m s^{-1} is reached inside the plasma nozzle, related to an average residence time, i.e., treatment time, of about 0.03 s. For particles with a diameter above 0.5 µm, the expansion vessel serves as an inertial separator. The main separating principles are deflection and deceleration of the gas stream. Due to a centrifugal acceleration of up to 50 m s^{-2}, particles with a diameter above 2 µm would be unable to follow the deflection of the gas stream at the bottom. The average residence time of the gas phase inside the expansion vessel is above 100 s which is more than sufficient for deceleration and separation of smaller particles. For particles with an aerodynamic diameter below 0.5 µm, diffusion separation applies through Brownian motion with particles attaching to the walls of the vessel. Although the particle size distribution is unknown, one can assume good separation rates for most particle sizes.

An alternating high-voltage Fourier synthesis pulse generator (Ingenieurbüro Dr. Jürgen Klein, S/N 040-3) with a pulse duration of 0.6 µs at adjustable peak voltage and repetition rate is connected to the dielectric isolated high-voltage electrode. The counter-electrode is linked to the ground potential.

Commercial test gas mixtures with 100 ppmv H_2S in N_2 (99.999 %; Westfalen AG, Germany) as well as synthetic biogas (50 % CO_2, 50 % CH_4, 50 or 100 ppmv H_2S; Westfalen AG, Germany) were supplied to the DBD devices via commercial thermal mass flow controllers (red-y smart GSC-C, Vögtlin Instruments AG).

The output gas composition was directly monitored via an online biogas analyzer (ExTox ET-8D). The analyzer is equipped with infrared channels for CH_4 and CO_2 and two electrochemical sensors for H_2S with an upper range of 100 and 3000 ppmv.

Additional analyses were conducted with a commercial system (MFM Analytical Systems, Multigas Analyzer MGA). For the quantitative analysis of the mass spectra, background spectra before starting the gas dosage were subtracted. Due to missing references for some species present within the spectra, especially ions, radicals, and metastables generated within the plasma, no correction for relative sensitivity factors or fragmentation intensities was included.

The chemical compositions at the surfaces of the sorbent powders were determined using a commercial Raman microscope (Senterra, Bruker Optik GmbH) equipped with a 532-nm laser light source and a sulfur reference (Fluka, Sulfur S_8, 99.999 %).

3 Results and Discussion

Earlier results on the removal of hydrogen sulfide from air streams [28] suggested a formation of $CaSO_4$, which has been verified in the meantime (not shown here). The formation of $CaSO_4$ from $CaCO_3$ and H_2S, however, requires additional oxygen in order to be completed. These positive results using sorbent powders should be extended towards an application for biogas desulfurization, investigated in the powder reactor (see Fig. 1). To exclude effects caused by humidity and further pollutants like terpenes and silanes, only synthetic biogas mixtures were employed.

3.1 Calcium Carbonate Sorbents in the Powder Reactor

The powder reactor was equipped with $CaCO_3$ powder for the conditioning of a biogas mixture of 50 % CO_2, 50 % CH_4, and approx. 50 ppm H_2S. The development of the H_2S concentration during the plasma treatment is illustrated in Fig. 3. The plasma reduced the H_2S content by about 65 %. However, the data points vary strongly by ± 15 ppm. The reason for this vari-

 © 2017 WILEY-VCH Verlag GmbH & Co. KGaA, Weinheim

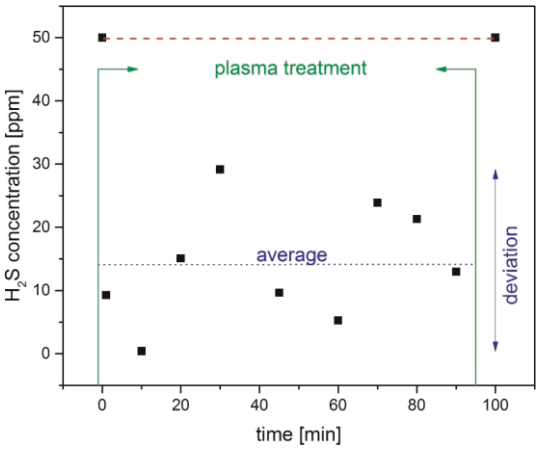

Figure 3. Development of the H_2S concentration over time within a biogas test mixture during plasma treatment including $CaCO_3$ sorbent powder.

ation can be understood when beholding the sorbent powder afterwards.

Fig. 4 depicts Raman spectra from the $CaCO_3$ powder sorbent after plasma treatment in a biogas mixture. For comparison, the spectra of pristine $CaCO_3$ powder (blue line) and a sulfur (S_8) reference powder (red line) are also given. The reaction product exhibits strong Raman bands of both $CaCO_3$ and S_8. However, no indications for $CaSO_4$ or other solid sulfur-containing compounds were found. The lack of oxygen in the biogas test gas hinders the formation of sulfate groups. Instead, the deposition of S_8 via dissociation of H_2S seems to occur. Further, this leads to the formation of H_2S via reverse reaction with gaseous hydrogen from earlier H_2S dissociation. These concurrent forward and reverse reactions are dependent not only on the earlier sulfur deposition onto the powder, but also on the gas flow conditions through the powder sorbent. All of these are continuously changing during operation of the plasma

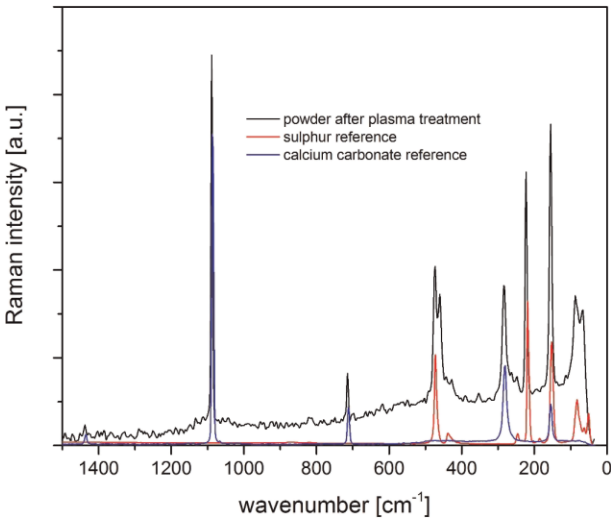

Figure 4. Raman spectra from a powder sorbent after plasma conditioning of a biogas mixture (black line) in comparison to pristine $CaCO_3$ (blue line) and sulfur (S_8) reference (red line).

reactor. For these reasons, the $CaCO_3$ powder is not suitable to be employed for the plasma-based removal of H_2S from biogas streams.

Similar experiments were conducted employing the iron(III) salts $FeCl_3$ and FeOOH (not shown). These compounds exhibit a spontaneous reactivity against H_2S, forming some FeS on the surface. However, the plasma was not able to improve these reactions. Instead, it only led to the dissociation of H_2S and thus to the deposition of atomic sulfur. Therefore, the further experiments focus on the use of this dissociation process for biogas purification purposes.

3.2 Powder Reactor without Powder Filling

Fig. 5 depicts the residual H_2S after plasma treatment in the powder reactor without any powder sorbent. Tests were done with a biogas mixture (50 % CO_2, 50 % CH_4, approx. 100 ppm H_2S) employing different pulse repetition rates, i.e., frequencies, and peak voltages. According to Penetrante and co-workers [29], the depletion of many gaseous pollutants in plasma processes follows an exponential behavior dependent on the amount of energy transferred into the working gas; c.f. also Schmidt et al. [31].

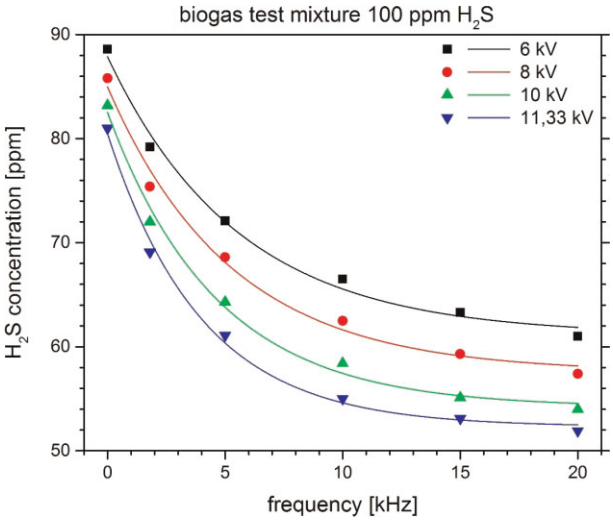

Figure 5. Residual H_2S content in a biogas mixture after plasma treatment at different frequencies and peak voltages.

Since the transferred energy is related to the peak voltage as well as the repetition rate, the results in Fig. 5 were fitted using an exponential function as given by Eq. (6).

$$p(H_2S) \sim e^{-V/\beta} \tag{6}$$

The resulting curves are displayed in Fig. 5 as solid lines. The H_2S content was reduced down to 61, 58, 54, and 52 ppm at decay constants β of 5.56, 5.24, 4.63, and 3.99 kHz for peak voltages of 6, 8, 10, and 11.33 kV, respectively. This supports the assumption that the desulfurization process via dissociation in DBD plasma depends mainly on the energy transferred into the gas stream.

 © 2017 WILEY-VCH Verlag GmbH & Co. KGaA, Weinheim

Fig. 6 illustrates the development of the CH_4 concentration in a biogas mixture versus the pulse repetition rates, i.e., frequencies, and peak voltages. A depletion of CH_4, e.g., via oxidation or polymerization [14, 15], was not detected but rather a minor increase in CH_4 content was found. Though results are very noisy, the data gives the impression of a linear dependence on the repetition rate, which corresponds to the energy transferred to the gas stream. Linear regressions yield slopes of 220, 350, 540, and 630 ppm kHz^{-1} at peak voltages of 6, 8, 10, and 11.33 kV, respectively. In contrast, the correlation between CH_4 increase and peak voltage is not linear.

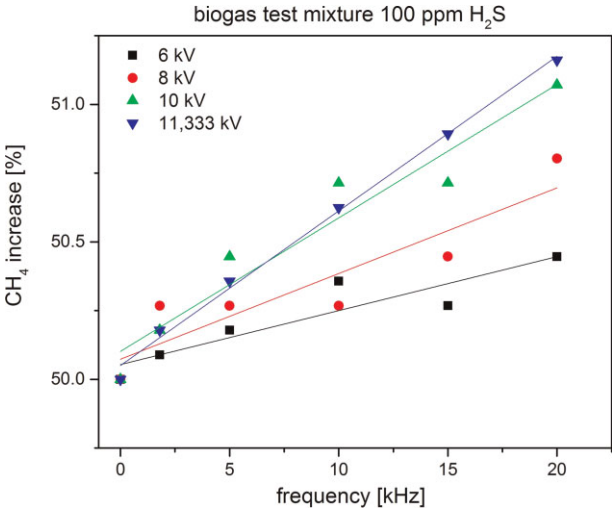

Figure 6. CH_4 concentration in a biogas mixture after plasma treatment at different frequencies and peak voltages.

This hydrogen for the CH_4 synthesis reaction according to the reaction

$$4\,H_2 + CO_2 \rightarrow CH_4 + 2\,H_2O \quad (7)$$

is partly supplied by the dissociation of H_2S [32]. However, the 50 ppm H_2S would certainly not be sufficient for the measured CH_4 increase of up to 1.3 vol %. The same applies for residual water fed with the gas stream. A possible redox reaction

$$CH_4 + CO_2 \rightarrow 2\,H_2O + 2\,C(s) \quad (8)$$

would lead to a proportionate reduction of both, methane and carbon dioxide, leading to precipitation of atomic carbon and production of water vapor. However, this can also be excluded, since there is neither an influence on the water content in the exhaust gas (additional mass spectra not shown), nor any sign of carbon within the sorbent powder; c.f. Raman spectra in Fig. 4. Thus, the H_2 source for the CH_4 production is not yet cleared out and needs further investigations.

The depletion of H_2S via dissociation as well as the production of CH_4 were verified for the powder reactor without any powder sorbent using different test gas mixtures and various techniques for gas analysis, again. The H_2S removal, however, severely suffered from the backwards reaction due to the sulfur deposited in the plasma region. Therefore, a new reactor system was developed in order to prevent the reverse reaction.

3.3 Plasma Nozzle with Expansion Vessel

The reactor used for the experiments described in the following combines a plasma nozzle and an expansion vessel to separate the sulfur from the plasma region and thus inhibit the backward H_2S formation reaction (see Fig. 2). Gas mixtures of 100 ppm H_2S diluted in N_2 were used to test the dissociation yields and the expected deposition of sulfur in the expansion vessel. The results for the residual H_2S content at different peak voltages and varying velocities of 1.56 (black squares), 3.13 (red circles), and 6.25 SLM (blue triangles) are summarized in Fig. 7.

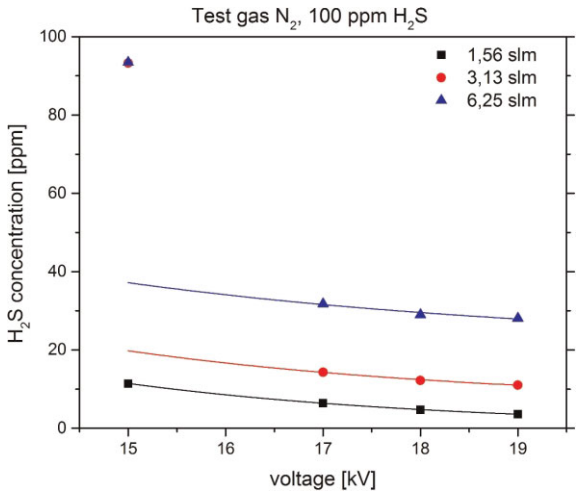

Figure 7. Voltage dependence of residual H_2S in N_2 after plasma processing at different gas velocities.

For 15 kV the plasma did not ignite stably, leading to several data points at an initial H_2S concentration of about 93 ppm. Fitting the data to exponential decay functions yields decay constants of 3.39, 3.85, and 4.79 kV for 1.56, 3.13, and 6.25 SLM, respectively. This indicates that higher voltages, i.e., larger powers are required at higher gas velocities. The reduction of 93 ppm H_2S down to 3.6 ppm at a proportionate production of H_2 (not shown in the figure) shows an effective dissociation of the H_2S. After the experiments, the vessel was covered with a yellow deposit, whereas only little debris could be found within the nozzle.

Fig. 8 presents a Raman spectrum of the solid substance from the expansion vessel (black line) compared to a sulfur S_8 reference (red line). The spectrum of the substance clearly resembles the sulfur reference as well as the stretching and bending vibrations of sulfur S_8 [30].

4 Conclusions

The formation of $CaSO_4$ from $CaCO_3$ and H_2S in an air plasma does not occur in oxygen-poor gases. Instead, a deposition of elemental sulfur (S_8) was found. For biogas, the presented powder reactor led to a plasma-driven reduction of H_2S by approx. 65 %. The residual H_2S content was highly fluctuating likely due to a significant backward reaction of the S_8 deposited on

 © 2017 WILEY-VCH Verlag GmbH & Co. KGaA, Weinheim

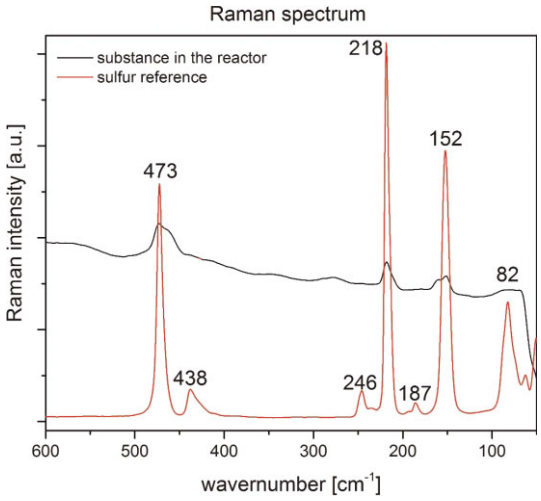

Figure 8. Raman spectra of yellow deposit found in the expansion vessel after desulfurization (black line) compared to a sulfur reference (red line).

the $CaCO_3$ powder. The reverse reaction obviously depends on the amount of sulfur and hydrogen present in the plasma as well as on the gas flow conditions.

Using powders with an intrinsic reactivity against H_2S like $FeCl_3$ and FeOOH, a spontaneous surface reaction forming FeS was found. This reaction, however, is self-constraint to only take place on the very surface. The activation by the plasma led to the reduction of H_2S at similar rates as for $CaCO_3$ powder, again depositing atomic sulfur (S_8). Fluctuations of the residual H_2S contents as well as the H_2S reformation were similar to the experiments employing $CaCO_3$ powder. Obviously, the use of powder sorbents is not preferred for the actual application as plasma-driven desulfurization of biogas.

An operation of the powder reactor without filling in any sorbent powder resulted in a removal of only about one-third of the H_2S at the same retention times and power supply. The influence of the peak voltage on the dissociation rate for H_2S was relatively low compared to the effect of the repetition rate of the pulses. Therefore, it is assumed that the reduced electric field strength due to the powder filling should also have a minor impact on the reaction rates. The main influence of the powder should then be given by its surface area, by which the possible number of adsorption sites would increase. These arguments are well supported by the significantly smaller fluctuation of the residual H_2S content when using the powder reactor without any filling.

Beside desulfurization, a notable production of CH_4 was observed which depends linearly on the energy density. The source of H_2, required to produce amounts of up to 1.3 vol % CH_4, however is not yet identified. The dissociation of H_2S might only lead to the formation of up to 100 ppm of H_2. Further tests have to be conducted to clarify these effects.

An optimized desulfurization reactor was implemented by combining a DBD plasma nozzle with a downstream expansion vessel. Here, dissociation of the H_2S takes place at high gas velocities inside the nozzle, but only few sulfur stuck to the nozzle walls whereas most of it accumulates in the expansion vessel. Due to this spatial separation of dissociation and deposition, the H_2S concentration could be reduced by around 96 %.

Acknowledgment

The authors gratefully acknowledge the financial support of the Alfred Kärcher Förderstiftung and Biothan GmbH. The authors also thank F. Endres and O. Höfft (Institute of Electrochemistry, Clausthal University of Technology) for the provision of the multi-gas analyzer and K. Bode (Institute of Inorganic and Analytical Chemistry, Clausthal University of technology) for the Raman measurements. The authors thank K. Kuzmicki for technical assistance.

The authors have declared no conflict of interest.

References

[1] A. Czernichowski, H. Lesueur, T. Czech, J. Chapelle, *ISPC-10*, Bochum, August **1991**.
[2] P. Adler, E. Billig, A. Brosowski, J. Daniel-Gromke, I. Falke, E. Fischer, J. Grope, U. Holzhammer, J. Postel, J. Schnutenhaus, K. Stecher, G. Szomszed, M. Trommler, W. Urban, *Leitfaden Biogasaufbereitung und -einspeisung* **2014**. http://mediathek.fnr.de/media/downloadable/files/samples/l/e/leitfaden_biogaseinspeisung-druck-web.pdf (Access on November 24, 2014).
[3] L. Vandenbulcke, S. de Persis, T. Gries, J. L. Delfau, *J. Taiwan Inst. Chem. Eng.* **2012**, *43*, 724–729. DOI: 10.1016/j.jtice.2012.03.006
[4] P. I. Khalaf, I. G. de Souza, E. Carasek, N. A. Debacher, *Quim. Nova* **2011**, *34*, 1491–1495.
[5] V. Goujard, J. M. Tatibouet, C. Batiot-Dupeyrat, *Appl. Catal., A* **2009**, *353*, 228–235. DOI: 10.1016/j.apcata.2008.10.050
[6] Y. N. Chun, Y. C. Yang, K. Yoshikawa, *Catal. Today* **2009**, *148*, 283–289. DOI: 10.1016/j.cattod.2009.09.019
[7] T. Nozaki, T. Hiroyuki, K. Okazaki, *Energy Fuels* **2006**, *20*, 339–345. DOI: 10.1021/er050141s
[8] U. Izquierdo, V. L. Barrio, K. Bizkarra, A. M. Gutierrez, J. R. Arraibi, L. Gartzia, J. Banuelos, I. Lopez-Arbeloa, J. F. Cambra, *Chem. Eng. J.* **2014**, *238*, 178–188. DOI: 10.1016/j.cej.2013.08.093
[9] B. Zhu, X. S. Li, J. L. Liu, X. B. Zhu, A. M. Zhu, *Chem. Eng. J.* **2015**, *264*, 445–452. DOI: 10.1016/j.cej.2014.11.112
[10] Y. N. Chun, S. W. Kim, H. O. Song, *Korean J. Chem. Eng.* **2004**, *21*, 670–675. DOI: 10.1007/BF02705503
[11] X. B. Zhu, K. Li, J. L. Liu, X. S. Li, A. M. Zhu, *Int. J. Hydrogen Eng.* **2014**, *39*, 13902–13908. DOI: 10.1016/j.ijhydene.2014.01.040
[12] T. Patipat, K. Parin, T. Nakorn, *Period. Polytech. Chem.* **2014**, *58*, 31–36. DOI: 10.3311/PPch.2114
[13] T. Kroker, *Ph.D. Thesis*, Technical University Carolo-Wilhelmina, Braunschweig **2011**.
[14] Y. Itoh, T. Oshita, K. Satoh, H. Itoh, *Electr. Eng. Jpn.* **2014**, *186*, 26–33. DOI: 10.1002/eej.22304
[15] T. Kolb, T. Kroker, K.-H. Gericke, *Vacuum* **2013**, *88*, 144–148. DOI: 10.1016/j.vacuum.2012.01.013

 © 2017 WILEY-VCH Verlag GmbH & Co. KGaA, Weinheim

[16] Y. Sekine, J. Yamadera, M. Matsukata, E. Kikuchi, *Chem. Eng. Sci.* **2010**, *65*, 487–491.
[17] L. Kolodkina, *Zh. Fiz. Khimii* **1935**, *6*, 428–435.
[18] U. Kogelschatz, E. Killer, B. Eliasson, *52nd Annu. Gaseous Electronics Conf.*, Norfolk, VA, October **1999**.
[19] E. Linga Reddy, V. M. Biju, C. Subrahmanyam, *Int. J. Hydrogen Eng.* **2012**, *37*, 2204–2209.
[20] Gutsol, T. Nunnally, A. Rabinovich, A. Fridman, A. Starikovskiy, A. Gutsol, A. Kemoun, *Int. J. Hydrogen Eng.* **2012**, *37*, 1335–1347.
[21] E. Linga Reddy, J. Karuppiah, C. Subrahmanyam, *J. Energy Chem.* **2013**, *22*, 382–386.
[22] H. Ma, P. Chen, R. Ruan, *Plasma Chem. Plasma Process.* **2001**, *21*, 611–624.
[23] H. Zhang, T. Ji, R. Zhang, H. Hou, *Plasma Sci. Technol.* **2012**, *14*, 134–139.
[24] Z. Li, H. Li'an, Y. Linsong, *Plasma Sci. Technol.* **2003**, *5*, 1961–1964.
[25] J. S. Herman, F. L. Terry, Jr., *J. Electron. Mater.* **1993**, *22*, 119–124.
[26] E. Linga Reddy, V. M. Biju, C. Subrahmanyam, *Int. J. Hydrogen Eng.* **2012**, *37*, 8217–8222.
[27] L. Zhao, Y. Wang, X. Li, A. Wang, C. Song, Y. Hu, *Int. J. Hydrogen Eng.* **2013**, *38*, 14415–14423.
[28] S. Dahle, *AIP Adv.* **2015**, *5*, 107234. DOI: 10.1063/1.4935102
[29] B. M. Penetrante, M. C. Hsiao, J. N. Bardsley, B. T. Merritt, G. E. Vogtlin, A. Kuthi, C. P. Burkhart, J. R. Bayless, *Plasma Sources Sci. Technol.* **1997**, *6*, 251–259.
[30] R. Streudel, *Spectrochim. Acta* **1974**, *31A*, 1065–1073.
[31] M. Schmidt, M. Schiorlin, R. Brandenburg, *Open Chem.* **2015**, *13*, 477–483.
[32] S. V. Kudryashov, A. Y. Ryabov, A. N. Ocheredko, K. B. Krivtsova, G. S. Shchyogoleva, *Plasma Chem. Plasma Process.* **2015**, *35*, 201–215.

 © 2017 WILEY-VCH Verlag GmbH & Co. KGaA, Weinheim

Research Article: $CaCO_3$, $FeCl_3$, and FeOOH were applied as powder sorbents for a plasma-based hydrogen sulfide removal from biogas mixtures. H_2S dissociation in dielectric barrier discharges proved to be effective for gas purification purposes. Medium high gas velocities in a nozzle-like plasma reactor and high retention times in a subsequent expansion vessel further enhanced the desulfurization efficiency.

Desulfurization of Biogas via Dielectric Barrier Discharges

M. Unseld, C. Szepanski, A. Lindermeir, W. Maus-Friedrichs, S. Dahle*

Chem. Eng. Technol. **2017**, *40 (2)*, XXX … XXX

DOI: 10.1002/ceat.201600282

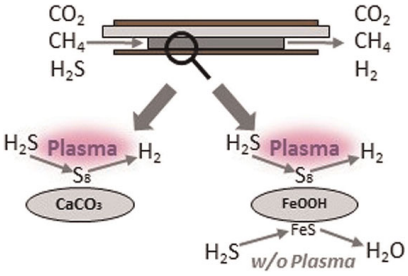

 © 2017 WILEY-VCH Verlag GmbH & Co. KGaA, Weinheim